

MPI-PhT/94-84
 LMU-23/94
 November 1994

Production Mechanisms for B_c Mesons in Photon–Photon Collisions¹

Karol Kołodziej^{a,2}, Arnd Leike^a and Reinhold Rückl^{a,b}

^a*Sektion Physik der Universität München,
 Theresienstr. 37, D-80333 München, FRG*

^b*Max-Planck-Institut für Physik, Werner-Heisenberg-Institut,
 Föhringer Ring 6, D-80805 München, FRG*

Abstract

Using photon-photon collisions as a particularly transparent study case we investigate the production mechanisms for B_c mesons. In nonrelativistic approximation and to $O(\alpha^2 \alpha_s^2)$ it is shown that recombination of \bar{b} - and c -quarks dominates by far over \bar{b} and c fragmentation. This dominance persists up to the highest accessible transverse momenta and leads to distributions in energy which differ completely from the spectra expected on the basis of the fragmentation functions. For processes in which a $b\bar{b}$ -pair is radiated from a primary c -quark, the fragmentation description is found to be inadequate. We anticipate important implications of these results for hadronic production of heavy quark resonances. Using realistic photon spectra we predict two-photon production rates for B_c and B_c^* at present and future e^+e^- -machines.

¹Supported by the German Federal Ministry for Research and Technology under contract No. 05 6MU93P.

² On leave from the Institute of Physics, University of Silesia, PL-40007 Katowice, Poland

1 Introduction

Since the top quark seems to be too short-lived for quarkonium-like resonances to form, the $\bar{b}c$ -bound states are most likely the only narrow heavy quark resonances besides the well-known charmonium and bottomonium systems. Till now these so-called B_c mesons have not yet been observed. However, they are expected to be in experimental reach with some luck already at LEP, more likely at the TEVATRON, but most certainly at the LHC. In addition, also the HERA-B experiment may get a glimpse on these very interesting bound states.

Because of flavour conservation in strong and electromagnetic processes, the B_c ground state can only decay weakly unlike the η_c and η_b . This fact provides unique possibilities to investigate important aspects of strong and weak interactions and their interplay. Indeed, the nonrelativistic nature of these systems allows to calculate also genuinely nonperturbative quantities such as total production cross sections, fragmentation functions, decay constants, and transition form factors. For this reason, the B_c system can serve as a testing ground for quantitative approaches to confinement problems and our understanding of soft hadron physics.

So far, the estimates only include the contributions of lowest order in the relative momentum of the constituent quarks and in the strong coupling constant. Moreover, they are subject to numerical uncertainties in the bound state wave functions, relevant quark masses and coupling constants. Independently of that, the calculations have not yet reached complete agreement on the hadronic production cross sections. Also, there are different opinions on the relative importance of recombination and fragmentation mechanisms, such as $\bar{b}c \rightarrow B_c$ and $\bar{b} \rightarrow B_c \bar{c}$, respectively.

In this paper, we take up the latter question and clarify the issue of recombination versus fragmentation. In order to liberate our study from unnecessary complications, we consider photon-photon instead of gluon-gluon scattering which is the dominant subprocess in hadronic collisions. The two reactions have many features in common including the competition of recombination and fragmentation processes. On the other hand, the absence of coloured quanta in the initial state of $\gamma\gamma$ -processes drastically reduces the number of Feynman diagrams at a given order and makes the calculations much more transparent. We realize, however, that the nontrivial colour coefficients in gg -processes somewhat change the relative weight of the different mechanisms in comparison to $\gamma\gamma$ -scattering.

Preliminary results of our study were already reported in ref. [1]. However, there the focus was more on the prospects of observing B_c mesons in e^+e^- -annihilation. Here, we complete our analysis of B_c production in $\gamma\gamma$ collisions and also correct a normalization error in the fragmentation estimate given in ref. [1]. Furthermore, we show the relevant differential distributions and point out the features which distinguish recombination from fragmentation. In addition, we examine in detail the theoretical validity of the factorized description in terms of heavy quark production, $\gamma\gamma \rightarrow c\bar{c}$ and $b\bar{b}$, and subsequent fragmentation, $c \rightarrow B_c b$ and $\bar{b} \rightarrow B_c \bar{c}$, respectively. Finally, we present predictions on the total cross section for B_c and B_c^* production in collisions of high energy photon beams which may be obtained by back-scattering of low energy, high intensity laser beams at future Linear Colliders, and in collisions of softer bremsstrahlung photons.

When our work was near to completion, a related study appeared in ref. [2]. If we use the same parameters we reproduce the total cross sections within the Monte Carlo uncertainties, except for the highest $\gamma\gamma$ c.m. energy of 100 GeV considered in ref. [2], where we disagree by ten per cent. Also the differential distributions presented in ref. [2] show in general the same behaviour as ours.

2 Classification of processes and calculation

In $\gamma\gamma$ collisions, B_c mesons are dominantly produced in association with a b - and c -quark jet,

$$\gamma(k_1) + \gamma(k_2) \rightarrow B_c(P) + b(p_b) + \bar{c}(p_c).$$

Here, the particle momenta are indicated in parentheses. To lowest order in the electromagnetic and strong coupling constants α and α_s , respectively, the above process is described by twenty Feynman diagrams. These can be classified in different topologies as indicated in Fig. 1. The diagrams belonging to set (I) can further be distinguished by the flavour of the primary quark line coupled to the photons. This line carries either the bottom (I_b) or the charm (I_c) flavour. The complete subsets of six diagrams with primary b - and c -quarks are found by interchanging the initial photons as required by Bose symmetry. These subsets are individually gauge invariant. The remaining eight diagrams belonging to set (II) are characterized by direct coupling of the initial photons to the two different quark flavours. The complete set (II) is obtained from the representative diagrams shown in Fig. 1 by interchanging independently the photons and quark flavours. Of course, also set (II) is by itself gauge invariant.

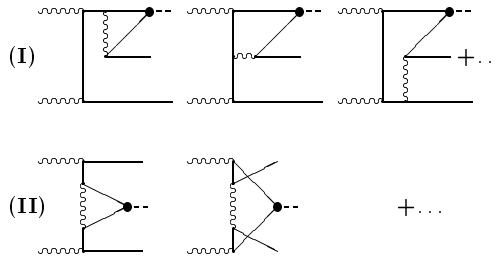


Fig. 1. *Different topologies of the lowest-order Feynman diagrams contributing to $\gamma\gamma \rightarrow B_c b\bar{c}$.*

More physically, the three subsets of diagrams discussed above can be interpreted as describing different production mechanisms. The subset (I_b) with primary b -quarks may be associated with $b\bar{b}$ production and \bar{b} -quark fragmentation $\bar{b} \rightarrow B_c \bar{c}$ in accordance with the first diagram of Fig. 1 (I). Similarly, one may be tempted to attribute the subset (I_c) to $c\bar{c}$ production followed by c -quark fragmentation $c \rightarrow B_c b$. However, while the fragmentation description

is applicable to the process (I_b), it does not hold for (I_c) as will be shown later. In contrast to the class (I) diagrams, the class (II) diagrams are characterized by direct production of a $b\bar{b}$ and $c\bar{c}$ pair from the initial photons and recombination of the \bar{b} - and c -quark into a B_c meson, $\bar{b}c \rightarrow B_c$. Obviously, the production amplitudes for the three different mechanisms are proportional to different combinations of the electric quark charges, namely $Q_b^2 = 1/9$, $Q_c^2 = 4/9$ and $Q_b Q_c = -2/9$, respectively. As one of the main results, we will show later that the recombination mechanism (II) dominates, while $b\bar{b}$ radiation from a primary c -quark (I_c) gives a small contribution and fragmentation of a primary \bar{b} -quark (I_b) is completely negligible.

We begin with a brief description of technical details of the calculation of amplitudes and cross sections. For definiteness and because of their particular importance, we concentrate on the pseudoscalar and vector ground states, B_c and B_c^* , respectively. Because of the nonrelativistic nature of these systems, the relative momentum p of the \bar{b} and c constituents and their binding energy are expected to be small in comparison to the quark masses. It is then reasonable to expand the amplitudes in p , and to keep only the lowest nonvanishing term [3]. In this approximation, the \bar{b} - and c -quark are on mass shell and move together with equal velocity. The following relations hold:

$$M(B_c) = M(B_c^*) = M = m_c + m_b, \quad p_c = \frac{m_c}{M} P, \quad p_{\bar{b}} = \frac{m_b}{M} P. \quad (1)$$

Moreover, the amplitudes for the production of S -waves reduce to hard scattering amplitudes multiplied by the S -wave function $\Psi(0)$ at the origin. For P -waves one obtains a similar product involving the derivative of the P -wave function. Using the definitions

$$\langle 0 | \bar{b} \gamma_\mu \gamma_5 c | B_c(P) \rangle = i f_{B_c} P_\mu \quad (2)$$

and

$$\langle 0 | \bar{b} \gamma_\mu c | B_c^*(P) \rangle = M f_{B_c^*} \epsilon_\mu \quad (3)$$

one can substitute the nonrelativistic wave function parameter $\Psi(0)$ by the corresponding decay constants

$$f_{B_c} = f_{B_c^*} = \sqrt{\frac{12}{M}} |\Psi(0)|. \quad (4)$$

As a simple rule, in the Feynman diagrams of Fig. 1 the transition from open quark production, $\gamma\gamma \rightarrow \bar{b}c\bar{b}\bar{c}$, to $B_c^{(*)}$ bound state production is achieved by making the following replacement [3]:

$$v(p_{\bar{b}})\bar{u}(p_c) = \frac{f_{B_c^{(*)}}}{\sqrt{48}} (\not{P} - M) \Pi_{SS_Z}. \quad (5)$$

Here, $v(p_{\bar{b}})$ and $\bar{u}(p_c)$ denote the Dirac spinors of the quarks forming the $B_c^{(*)}$ bound states, and Π_{SS_Z} is the appropriate spin projector, $\Pi_{00} = \gamma_5$ for pseudoscalars and $\Pi_{1S_Z} = \not{\epsilon}$ for vectors. In Fig. 1, this formal substitution is indicated by the dark dot. Obviously, because of the neglect of the relative momentum of the constituent quarks, the Feynman amplitudes involve no loop in momentum space, but only traces of Dirac and colour matrices. Note that the colour structure is not accounted for in eq. (5). All diagrams of Fig. 1 have the same colour factor $\frac{4}{3}$ which has been included in the overall normalization of the cross sections.

The squared matrix element is obtained by two independent methods. One calculation is based on the traditional trace technique. The necessary traces are calculated using the symbolic

manipulation program **FORM** [4]. The resulting expressions are automatically implemented into a **FORTRAN** program. The second calculation is based on a generalization of the method described in detail in ref. [5] for bosonic final states in e^+e^- scattering. Here, the polarized matrix elements are calculated in a fixed Lorentz frame using the Weyl representation of the Dirac matrices and spinors together with real polarization vectors. The matrix element is reduced analytically to a linear combination of products of the 2×2 Pauli matrices. These products are computed numerically. The use of real photon polarization vectors allows to reduce the number of elements of the matrices which have to be calculated by a factor of two. The polarized matrix elements are obtained by sandwiching these matrices between 2×2 Pauli spinors. As the last step, one sums over polarizations. The matrix elements squared obtained by the two methods agree to ten digits.

The phase space integration is also performed independently using two different routines. Before employing the Monte Carlo integration routine **VEGAS** [6] the strongest peaks of the matrix elements were eliminated by introducing new integration variables. After the integration all differential distributions and cross sections agree within the Monte Carlo errors.

3 Results

For numerical purposes and all subsequent figures, we choose the following values of the parameters:

$$m_b = 4.8 \text{ GeV}, \quad m_c = 1.5 \text{ GeV}, \quad \alpha_s = 0.2, \quad \alpha = 1/129, \quad f_{B_c} = f_{B_c^*} = 0.4 \text{ GeV} \quad [7]. \quad (6)$$

In Fig. 2 we compare the cross section $\sigma(I_b + I_c + II)$ for $\gamma\gamma \rightarrow B_c b\bar{c}$ derived from the complete set of $O(\alpha^2 \alpha_s^2)$ diagrams indicated in Fig. 1 with the cross sections $\sigma(I_b)$ and $\sigma(I_c)$ resulting from the gauge invariant subset (I) with primary b - and c -quarks, respectively. Also shown are the results obtained by simply multiplying the cross sections $\sigma_{b\bar{b}}$ and $\sigma_{c\bar{c}}$ for open flavour production with the respective fragmentation probabilities $P(\bar{b} \rightarrow B_c \bar{c})$ and $P(c \rightarrow B_c b)$ [8]. These probabilities have been calculated separately in the same nonrelativistic approximation as described in section 2.

As can be seen, the total production cross section is dominated by the recombination mechanism except very near to the production threshold, where also fragmentation, or more precisely radiation, processes give significant contributions. Moreover, it is more efficient to produce a pair of c -quarks and to radiate from them a $b\bar{b}$ -pair in order to form a B_c meson than to produce a pair of b -quarks and to radiate a $c\bar{c}$ -pair. The reason is the electric charge of the primary quarks which yields a factor 16 in favour of c -quarks. Finally, the factorized description in terms of open flavour production, $\gamma\gamma \rightarrow b\bar{b}$ and $\gamma\gamma \rightarrow c\bar{c}$, followed by the fragmentation processes, $\bar{b} \rightarrow B_c \bar{c}$ and $c \rightarrow B_c b$, respectively, provides a good approximation to the class (I) processes only when the primary quark is a b -quark, but not when it is a c -quark. These findings are in sharp contrast to B_c production in e^+e^- -annihilation [9, 10]. There, the recombination mechanism is absent and the radiation of a $b\bar{b}$ pair from primary c -quarks is negligible. Furthermore, the fragmentation picture works perfectly no matter whether the fragmenting quark is the heavier or the lighter one.

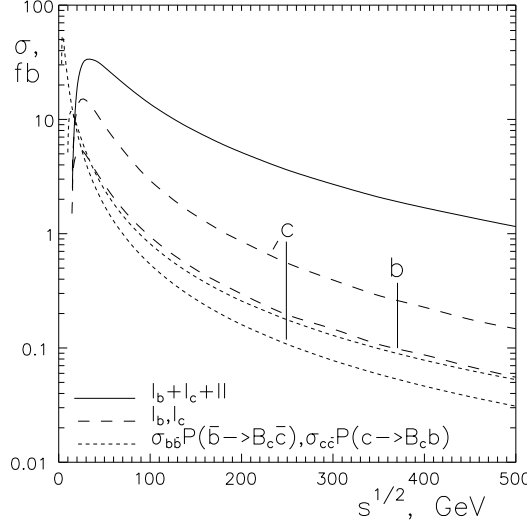


Fig. 2. Integrated cross sections for $\gamma\gamma \rightarrow B_c b\bar{c}$ versus the c.m. energy. The different calculations are explained in the text. The production mechanisms are as classified in Fig. 1.

We have investigated the break-down of the fragmentation description for the class (I) processes in $\gamma\gamma$ -scattering in some more detail. In energy range considered, this approximation is indeed only applicable when the fragmenting quark is appreciably heavier than the quark flavour produced via gluon radiation. Such a favourable case is illustrated in Fig. 2 by $\sigma(I_b)$ and $\sigma_{b\bar{b}}P(\bar{b} \rightarrow B_c \bar{c})$ which agree nicely. However, already for equally heavy quarks, a case realized in the analogous process $\gamma\gamma \rightarrow J/\psi c\bar{c}$, we find considerable disagreement. To be more definite, $\sigma(\gamma\gamma \rightarrow J/\psi c\bar{c})/\sigma_{c\bar{c}}2P(\bar{c} \rightarrow J/\psi \bar{c}) \approx 2.1$ (1.4) at $\sqrt{s} = 20$ (500) GeV. When the fragmenting quark is the lighter one, the fragmentation description fails completely as demonstrated by $\sigma(I_c)$ and $\sigma_{c\bar{c}}P(c \rightarrow B_c b)$ in Fig. 2. It is the second diagram of Fig. 1 (I) which seems to be responsible for the break-down of factorization. This diagram is absent in e^+e^- annihilation, but it is necessary in $\gamma\gamma$ -scattering for gauge invariance.

Further features of the different production mechanisms and theoretical descriptions can be learned from differential distributions of the B_c mesons. Fig. 3 shows the distributions in the scaled energy variable $z = 2E_{B_c}/\sqrt{s}$ obtained from the complete set of $O(\alpha^2\alpha_s^2)$ diagrams and from the gauge-invariant subsets (I_b) and (I_c) alone. Most notably, the dominant recombination processes populate the soft end of the spectrum, while the class (I) processes give rise to a characteristic high energy tail. The hard component (I_b) is as expected from b -quark fragmentation. In fact, the energy distribution predicted from the diagrams of class (I_b) is practically indistinguishable from the corresponding fragmentation function $D_{\bar{b} \rightarrow B_c}(z)$ [8, 10]. However, for the component (I_c) the analogous distributions do not coincide. The actual energy spectrum derived from the diagrams (I_c) is considerably harder than the fragmentation function $D_{c \rightarrow B_c}(z)$ [8, 10]. The above assertions are illustrated more clearly in Fig. 4 where we plot the individual energy spectra generated by the processes (I_b), (I_c) and (II) in comparison to the fragmentation functions $D_{\bar{b} \rightarrow B_c}(z)$ and $D_{c \rightarrow B_c}(z)$. Here, all distributions are normalized to unity.

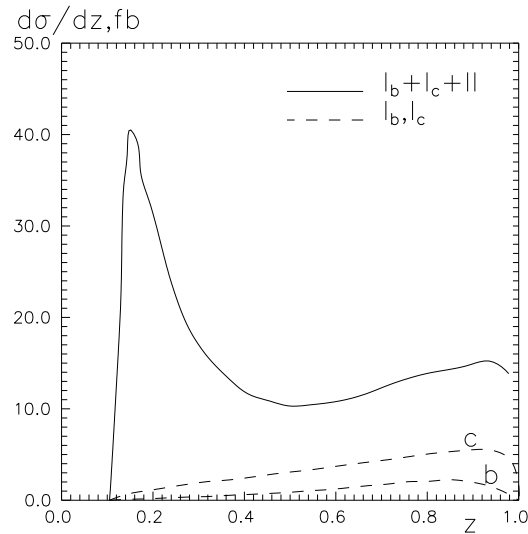


Fig. 3. Energy distributions of B_c mesons at $\sqrt{s} = 100$ GeV with all processes of Fig. 1 included and from the radiative mechanisms (I_b) and (I_c) alone.

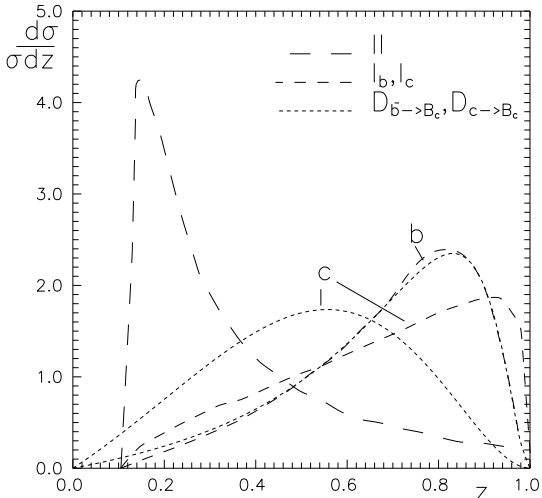


Fig. 4. Normalized energy spectra of B_c mesons at $\sqrt{s} = 100$ GeV generated by the mechanisms (II), (I_b) and (I_c) of Fig. 1 in comparison to the heavy quark fragmentation functions.

Interesting observations can also be made from the p_T distributions depicted in Fig. 5. The factorized description in terms of $b\bar{b}$ production and \bar{b} -fragmentation and the corresponding diagrams (I_b) of Fig. 1 yield distributions which are very similar in shape and normalization except in the low- p_T region. As far as the shape is concerned this is even true for the analogous processes with primary c -quarks. However, the c -quark fragmentation picture fails to reproduce the correct magnitude of the cross section for the process (I_c), a problem already noticed in Fig. 2. We also see that the radiation of a $c\bar{c}$ -pair from a b -quark leads to a harder p_T distribution for the B_c bound states than the radiation of a $b\bar{b}$ -pair from c -quarks. Finally, the most important observation is that the recombination mechanism dominates B_c production not only at low p_T , as one could have expected, but also in the high- p_T region up to the kinematic limit. In other words, the familiar description of high- p_T hadron production in terms of the production and fragmentation of quarks with large transverse momenta is inadequate for single B_c production in $\gamma\gamma$ -scattering and similar processes.

For completeness, we mention without showing figures that the angular distributions resulting from the different mechanisms considered above are all quite similar in shape. The distributions are sharply peaked in forward and backward direction, with the distribution predicted by the complete set of diagrams of Fig. 1 being slightly flatter than the distributions derived from subsets (I_b) and (I_c), and from b - and c -quark fragmentation.

So far we have concentrated on the problem of identifying the dominant production mechanisms and examining different theoretical descriptions. For this purpose, it is sufficient to consider photon-photon collisions at fixed energies. Now we want to make predictions on the production rates of B_c mesons in photon-photon collisions at e^+e^- -machines in the LEP energy range and beyond. To this end we fold the total cross sections for $\gamma\gamma \rightarrow B_c^{(*)}b\bar{c}$ with realistic photon spectra that is the photon spectrum obtained by Compton back-scattering of high intensity laser light on e^\pm beams [11], or the Weizsäcker-Williams bremsstrahlung spectrum

[12]. Our results are shown in Fig. 6, where we have plotted the convoluted cross sections for production of the pseudoscalar and vector ground states versus the e^+e^- centre-of-mass energy. For reference we also show the unfolded cross sections for the subprocesses $\gamma\gamma \rightarrow B_c^{(*)}b\bar{c}$ as functions of the $\gamma\gamma$ centre-of-mass energy. As expected from the shape of the Compton spectrum which has a long tail towards soft photons, and the shape of the $\gamma\gamma$ -cross section which peaks just above threshold, the convolution increases the cross sections substantially for energies above 100 GeV. At a 500 GeV linear collider and for an integrated luminosity of 10 fb^{-1} , one can produce about 100 B_c and 400 B_c^* mesons. In contrast, the yield of B_c mesons from bremsstrahlung photons is very small at LEP energies, but increases logarithmically with energy. While at LEP 2 the production rate is still too low to lead to observable signals, in the TeV energy range bremsstrahlung photons become competitive with back-scattered laser photons in producing B_c mesons.

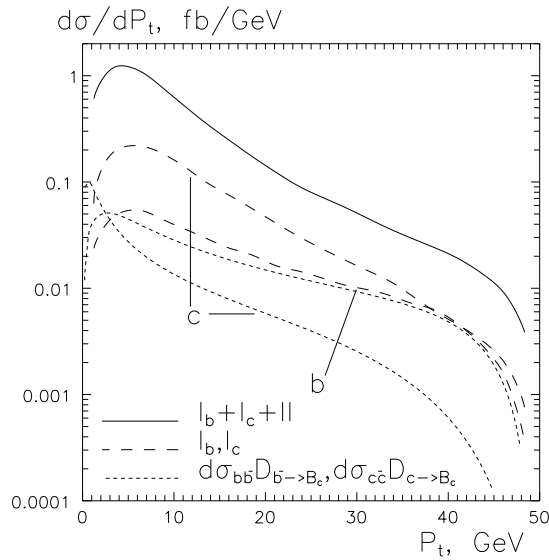


Fig. 5. The B_c transverse momentum distributions at $\sqrt{s} = 100$ GeV for the different mechanisms and descriptions considered in Fig. 2.

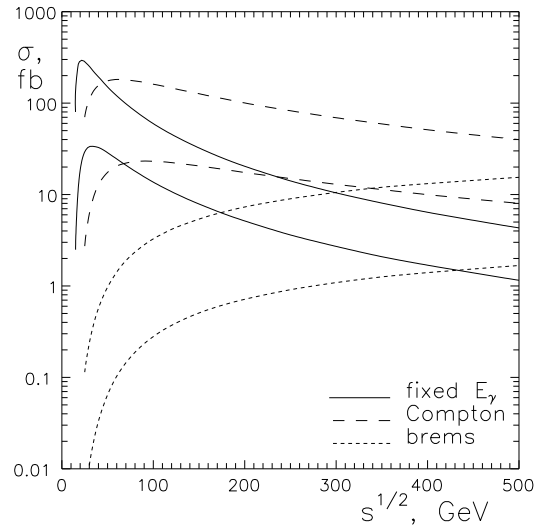


Fig. 6. Total production cross sections for B_c^* (upper curves) and B_c (lower curves) versus the $\gamma\gamma$ c.m. energy (full), and convoluted with the Compton spectra of back-scattered laser light (long-dashed) and with bremsstrahlung spectra (short-dashed) versus the e^+e^- c.m. energy.

4 Summary

We have studied the production of B_c mesons in photon-photon scattering. Our main results can be summarized as follows. The dominant production mechanism proceeds via direct coupling of a $b\bar{b}$ and $c\bar{c}$ pair to the initial photons and recombination of the \bar{b} - and c -quark into the B_c bound state. The radiative process where a $c\bar{c}$ -pair is produced via gluon emission

from a primary b -quark plays a negligible role. It is well described by b -quark production and fragmentation, $\gamma\gamma \rightarrow b\bar{b}$, $\bar{b} \rightarrow B_c\bar{c}$. The analogous process where a $b\bar{b}$ -pair is emitted from a primary c -quark is enhanced by the charge ratio Q_c^4/Q_b^4 , but it still plays a marginal role. Here, the fragmentation description $\gamma\gamma \rightarrow c\bar{c}$, $c \rightarrow B_c b$ does not hold.

Given the dominance of recombination even at large transverse momenta up to the kinematic limit we conclude that the usual hard scattering formalism in terms of high- p_T quark production and subsequent fragmentation cannot be applied to $\gamma\gamma \rightarrow B_c X$. This also puts serious doubts on the calculations of hadronic B_c [13] and J/ψ [14] production based on $b\bar{b}$ and $c\bar{c}$ production via gluon-gluon fusion followed by heavy quark fragmentation. Although the replacement of the electric charges by colour charges when going from $\gamma\gamma$ - to gg -processes changes the relative weights of the production mechanisms considered in this paper, we suspect the fragmentation description to underestimate the yields of heavy bound states in the experimentally accessible, high- p_T regime.

The $B_c^{(*)}$ production rates predicted for $\gamma\gamma$ collisions and realistic photon energy distributions show that these processes are below the observability limit in e^+e^- -collisions at LEP energies. However, at linear colliders in the TeV energy range, two-photon production of B_c mesons may come into experimental reach. These general prospects are little affected by the sizeable uncertainties in the values of parameters quoted in eq. (6), and the unknown higher order perturbative, nonperturbative and relativistic corrections.

References

- [1] A. Leike, R. Rückl, Nucl. Phys. B (Proc. Suppl.) **37B** (1994) 215.
- [2] A.V. Berezhnay, A.K. Likhoded, M.V. Shevlyagin, hep-ph 9408287.
- [3] B. Guberina, J.H. Kühn, R.D. Peccei, R. Rückl, Nucl. Phys. **B174** (1980) 317.
- [4] J.A.M. Vermaasen, *Symbolic Manipulation with FORM version 2, Tutorial and Reference Manual CA*, Amsterdam, 1991.
- [5] K. Kołodziej, M. Zrałek, Phys. Rev. **D43** (1991) 3619.
- [6] G.P. Lepage, J. Comp. Phys. **27** (1978) 192.
- [7] S. Reinshagen, diploma thesis, Univ. of Munich, 1991; S. Reinshagen, R. Rückl, in Proc. of the Workshop on Quantum Field Theoretical Aspects of High Energy Physics, eds. B. Geyer, E.-M. Ilgenfritz, Univ. of Leipzig, 1993.
- [8] E. Braaten, K. Cheung, T.C. Yuan, Phys. Rev. **D48** (1993) 4230; R5049.
- [9] L. Clavelli, Phys. Rev. **D26** (1982) 1610; C.-R. Ji, R. Amiri, Phys. Rev. **D35** (1987) 3318; V. Barger, K. Cheung, W.-Y. Keung, Phys. Rev. **D41** (1990) 1541; C.-H. Chang, Y.-Q. Chen, Phys. Lett. **B284** (1992) 127.
- [10] F. Amiri, C.-R. Ji, Phys. Lett. **B195** (1987) 593; C.-H. Chang, Y.-Q. Chen, Phys. Rev. **D46** (1992) 3845.

- [11] I.F. Ginzburg, G.L. Kotkin, V.I. Telnov, Nucl. Instr. Meth. **205** (1983) 47; V.I. Telnov, in Proc. of the IXth Int. Workshop on Photon-Photon Collisions, eds. D.O. Caldwell, H. P. Paar (World Scientific, Singapore, 1992) p. 369.
- [12] C. F. Weizsäcker, Z. Phys. **88** (1934) 612; E. J. Williams, Phys. Rev. **45** (1934) 729.
- [13] K. Cheung, Phys. Rev. Lett. **71** (1993) 3413.
- [14] D. P. Roy, K. Sridhar, CERN-TH.7329/94.